Increased tolerance to organic xenobiotics following recent allopolyploidy in Spartina (Poaceae)

Armand Cavé-Radet, Armel Salmon, Oscar Lima, Malika Ainouche, Abdelhak El Amrani

Title: Increased tolerance to organic xenobiotics following recent allopolyploidy in *Spartina* (Poaceae)

Authors: Armand Cavé-Radet[1], Armel Salmon[1], Oscar Lima[1], Malika L. Ainouche[1] and Abdelhak El Amrani[1]†

[1]Université de Rennes 1, OSUR/CNRS-UMR 6553, Ecosystèmes-Biodiversité-Evolution, Campus de Beaulieu, Bâtiment 14A, 35042 Rennes cedex, France.

† Corresponding author: Abdelhak El Amrani (Email: abdelhak.elamrani@univ-rennes1.fr)
Université de Rennes 1
Centre National de la Recherche Scientifique
UMR 6553 Ecosystems-Biodiversity-Evolution
Campus de Beaulieu, Bâtiment 14A
263 avenue du Général Leclerc
F-35042 Rennes Cedex, France

Highlights:

- First PAH tolerance comparative analyses in *Spartina*.
- Increased tolerance highlighted in the allopolyploid *S. anglica* compared to its parents.
- Expression analysis of candidate GST genes (*Tau* family related) in *Spartina.*
- Allopolyploidization and phenanthrene induced stress reprogrammed GST gene expression patterns.
- The neoallopolyploid *S. anglica* is a suitable candidate for phytoremediation.

Abstract

Genome doubling or polyploidy is a widespread phenomenon in plants where it has important evolutionary consequences affecting the species distribution and ecology. PAHs are ubiquitous organic pollutants, which represent a major environmental concern. Recent data showed that tolerance to organic xenobiotics involve specific signaling pathways, and detoxifying gene sets referred as 'the xenome'. However, no data are available about how polyploidy impacts tolerance to organic xenobiotics. In the present paper, we investigated PAH tolerance following allopolyploidization in *Spartina alterniflora*, *S. maritima* and their derived allopolyploid species *S. anglica*. We performed comparative analyses of cellular compartmentalization, photosynthetic indices, and oxidative stress markers under phenanthrene-induced stress, and found that *S. anglica*

exhibit increased tolerance compared to its parents. Based on 52 genes potentially involved in phenanthrene detoxification previously identified in *A. thaliana,* we investigated the *Spartina* xenome using genomic and transcriptomic available resources. Subsequently, we focused on GSTs, a ubiquitous enzymes class involved in organic xenobiotic detoxification. We examined expression profiles of selected genes by RT-qPCR, and revealed various patterns of parental expression alteration in the allopolyploid. The impacts of allopolyploidization on phenanthrene-induced stress and their potential ecological implications are discussed. The neo-allopolyploid *S. anglica* appears as a potential candidate for phytoremediation in PAH-polluted marshes.

Key words: Genome doubling, PAHs, abiotic stress, GSTs, *Spartina*

1. INTRODUCTION

Whole genome duplication (WGD, or polyploidization) is an important mechanism in plant evolutionary history [1]. Polyploidy is accompanied by significant structural and functional genome reorganizations, which may affect the adaptive dynamics of newly formed species (*e.g.* larger habitats, increased fitness) [2–5]. In allopolyploids, both genome merger ("genomic shock" resulting from interspecific hybridization) and genome redundancy (resulting from genome doubling *per se*) result in novel genetic and epigenetic interactions, affecting the subsequent evolution and adaptation of species [6].

In this paper, we explore the hypothesis of increased stress tolerance to organic xenobiotics following allopolyploidy in *Spartina* species. *Spartina* is a monophyletic lineage that was recently included in the former paraphyletic genus *Sporobolus* [7]. This lineage is affected by recurrent hybridization and genome duplication, and includes 13 to 15 perennial species colonizing estuaries, coastlines and continental wetlands worldwide. Three species are of particular ecological and evolutionary interests: the European native *S. maritima* (Curtis) Fernald (2n = 6x = 60), the recently introduced to Europe from eastern America *S. alterniflora* Loisel. (2n = 6x = 62), and the allopolyploid *S. anglica* C. E. Hubbard (2n = 12x = 120, 122 or 124). *Spartina alterniflora* (maternal parent) hybridized with *S. maritima* (paternal parent) which resulted in the formation of a sterile F1 hybrid *S. x townsendii,* discovered in 1870 (H. Groves & J. Groves; 2n = 6x = 62). A few decades later (around the 1890's), chromosome doubling of this hybrid led to the formation of a new fertile and vigorous allododecaploid species *S. anglica* (see Supplemental Fig. S1), now being listed among the 100 worst invasive alien species (IUCN list [8]). *Spartina anglica* represents a classic example of recent allopolyploid speciation in natural environments, and an excellent system to explore the immediate consequences of allopolyploidy in a well-established historical and phylogenetic framework [9–11]. Hence, when comparing *S. anglica* to its parents, several studies [12–15] highlighted gene expression evolution, and epigenetic modifications such

as DNA methylation alterations. *Spartina* species are regularly confronted with fluctuating environments: they are able to tolerate several hours of submersion in seawater, thanks to a developed aerenchyma [16] and efficient 'anaerobic respiration' capabilities [17]. They are also strongly tolerant to flooding [16,17], salt stress [18] and chemical pollution (*e.g.* PAHs, crude oil, heavy metals; see [19–24]).

Spartina species are recurrently exposed to oil spills [20,24]. In this context, we argued that allopolyploidy might contribute to *Spartina* tolerance to abiotic stress, such as tolerance to PAHs (Polycyclic Aromatic Hydrocarbons). PAHs are ubiquitous organic pollutants which represent a major concern in terms of ecotoxicology and public health [25–27]. PAH plants detoxification mechanisms are still poorly understood, but studies reported that plants are able to absorb, metabolize and/or degrade PAHs. Most organic xenobiotics are taken up by plant roots from soil, and translocated through the xylem to the shoot system for compartmentation and degradation [28,29]. Indeed, the uptake of PAHs by plant roots occurs through simple diffusion [29] or active transport [30].

In response to PAHs, plants are experiencing xenobiotics toxicity and associated oxidative stress damages. Xenobiotics affect the plant physiology by reducing major metabolic functions such as photosynthesis and respiration [31–33]. Moreover, PAHs are described to induce oxidative stress, through ROS (Reactive Oxygen Species) accumulation in plant cells, which in turn reduce plant development and growth, chlorophyll levels, and lead to trichome deformation and necrosis [31,32,34]. Oxidative stress damages induced by ROS under PAH stress are balanced by antioxidant enzymes, that are most likely limiting xenobiotic tolerance abilities [32]. More specifically, Dumas *et al.* [35] found that PAH accumulation in leaves inhibits electron transfer and photosynthesis within a few minutes, disrupting the energy transformation. Additionally, a microarray-based transcriptional profiling has established transcriptional reprogramming in *Arabidopsis* exposed to PAH [35,36]. These investigations under PAH-induced stress highlighted the importance of plant hormones such as ethylene [36] and other secondary metabolites [37] involved in defense pathways.

Introduced by Edwards *et al.* [38], the concept of 'xenome' was developed to characterize genes involved in tolerance mechanisms and metabolization of xenobiotics. In *Arabidopsis*, transcriptomic analysis under PAH-induced stress (plantlets exposed to phenanthrene) led to the identification of a gene set potentially involved in PAH sensing and detoxification [35]. PAH transformation involves oxidoreductases and hydrolases (including cytochromes P450: CYPs, peroxidases, dioxygenases and carboxylesterases) for xenobiotic solubilization. PAHs are then conjugated to endogenous molecules by the intervention of transferases, including glutathione-S-

transferases (GSTs), glycosyltransferases (GTs) and malonyltransferases (MTs). These transformed molecules are then either neutralized by partnering with cell wall polymers such as lignin, stored in the vacuole through ATP-binding cassette (ABC) transporters, or exported out of the cell [39,38]. Plant response to xenobiotics occurs rapidly, and can be divided into three phases as (1) perception and signaling, (2) detoxification, and (3) degradation [40,35]. Most of our knowledge of the molecular and physiological mechanisms involved in xenobiotic tolerance relies on model systems such as *Arabidopsis*. Recently, Alvarez *et al.* [41] performed transcriptome profiling of resilient *S. alterniflora* natural populations exposed to crude oil, that provided some candidate genes involved in xenobiotic detoxification mechanisms.

In the present paper, we explored the *Spartina* model in order to examine the impact of interspecific hybridization and whole genome duplication (allopolyploidization) in the establishment of tolerance mechanisms to phenanthrene. Hence, we conducted comparative analyses of physiological changes in the parental species and the allopolyploid *S. anglica* under phenanthrene-induced stress, quantification and histochemical localization in leaf tissues. In parallel, we assessed changes of oxidative stress, and photosynthetic capacity (chlorophyll fluorescence) under phenanthrene-induced stress, and analyzed transcriptional changes of candidate genes involved in PAH detoxification pathways. The impact of allopolyploidy is subsequently discussed.

2. MATERIALS AND METHODS

2.1. Plant materials

We collected plants in various locations along the Brittany coastline (France). We sampled *S. alterniflora* in Hopital-Camfrout (Finistère, France), whereas *S. maritima* and *S. anglica* were collected at Le Hezo (Morbihan, France). We maintained plants transplanted in pots containing a mixture of soil and sand (70 % and 30%, respectively) in the greenhouse, under fluorescent light/dark regime of 16/8h, and an average ambient temperature of 20°C.

2.2. *In vitro* experimental design: culture conditions and phenanthrene treatments

As germination of *Spartina* seeds is problematic (most particularly in *S. maritima*), we designed an *in vitro* protocol, using square leaf portions (0.5-1 cm large) placed in Petri dishes (15×15 cm). We used phenanthrene (phe: $C_{14}H_{10}$), which is commonly reported as a PAH representative molecule. The molecular structure of phenanthrene is composed of three fused benzene rings,

resulting in a low molecular weight, and efficient plant uptake. In crude oil, phenanthrene may represent up to 17% of total PAHs [42].

First, we incubated leaf tissues for 5 min in sodium hypochlorite (1.25% active chlorine), and rinsed successively three times during 5 min in sterile water. We prepared Petri dishes with a solid growth medium (half-strength Murashige and Skoog: 0.5 MS; 0.8% agar; pH= 5.6). These media were supplemented or not with phenanthrene from a stock solution dissolved in absolute ethanol at 200 mM, reaching concentrations of 0, 100 and 400 µM phe. Such treatments allowed us to compare stress tolerance levels between species (control and phenanthrene-induced stress conditions), or to assess more precise dose-response effects. We added identical volumes of ethanol alone to controls. This simplified procedure provides an optimal control of experimental conditions, phenanthrene being assimilated by foliar uptake, as explained by Smith and Jones [43]. We cultivated foliar tissues in Petri dishes in a phytotronic chamber with light/dark regime of 16/8h, temperature 22/18°C. We conducted all experiments in three biological and technical replicates.

2.3. Phenanthrene histolocalisation and quantification in foliar tissues

2.3.1. Phenanthrene histolocalisation

We performed microscopic observations at the Cell Imaging platform (INRA Toulouse, France) on semi-thin sections of leaves treated with 0 and 400 µM phe. Per treatment, we observed sections from nine leaf fragments by species (three biological replicates from distinct plants and technical triplicates). Phenanthrene fluorescence was detected using epifluorescence microscopy (Axiozoom V16, Zeiss). We also analyzed samples by confocal microscopy (LEICA SP2), by scanning along different wavelengths in the visible spectrum to identify specific emissions for phenanthrene and cellular components. Exited at 253 nm, chlorophylls are observed in red, and phenanthrene in blue (emitting around 430 and 455 nm). Phenanthrene fluorescence is distinguished from lignin autofluorescence which specifically emit at 472 nm (see Supplemental Fig. S2). Then, we used three-dimensional fluorescent reconstructions of leaf tissues to identify and specifically locate the xenobiotic into the cellular matrix.

2.3.2. Phenanthrene quantification

We estimated phenanthrene contents in *Spartina* tissues on leaf portions treated under 100 µM phe. We first rinsed the harvested plant material (around 200 mg of leaf tissues from at least three fragments from biological triplicates) in absolute ethanol and in distilled water. Samples were lyophilized for 72h, before being ground and weighted. We extracted organic matter samples

using an accelerated solvent extractor (ASE 200, Dionex) with dichloromethane at 100°C under pressure. After evaporation, we diluted extracts with dichloromethane, and added quantification standards. Thereafter, we first performed fractionation by liquid chromatography, then we proceeded to identification and quantification of phenanthrene by gas chromatography and mass spectrometry (GC-MS).

2.4. Physiological and biochemical analyses

2.4.1. Chlorophyll fluorescence

We quantified chlorophyll fluorescence using a pulse amplitude-modulated fluorometer (Junior-PAM, Walz GmbH; Effeltrich, Germany). The device delivers a saturating pulse through a light guide; and collects different parameters related to the plant photochemistry. Photon absorption by chlorophyll molecules occurred at the excited state. By returning to their basal state, the resulting energy dissipated by the chlorophyll is either used for photosynthesis, dissipated as heat or re-emitted as fluorescence [44]. These three processes are closely related to each other. Thus, determining a change in chlorophyll fluorescence is equivalent to identify a change in the yield of photochemical photosystem. Here we focus on photosystem II (PS II) and most particularly on two parameters as indices of photosynthetic capacity: *Fo* (basic fluorescence yield) and *Fm* (maximal fluorescence yield). These indices represent minimum and maximum fluorescence values where reaction centers of PS II are respectively activated and inactivated, and *Fv* is defined as the difference between the two indices as the maximum variable fluorescence (*Fv = Fm-Fo*). *Fv*/*Fm* normalized ratio is used to approximate the maximum photochemical quantum yield of PS II, to assess photosynthetic apparatus status in response to stress.

We performed measurements on leaf fractions (nine foliar fragments from biological and technical triplicates) cultivated 10 days under phenanthrene treatments (0, 100 and 400 µM), and acclimated for 30 min in the dark before measurements, preventing PS II activity.

2.4.2. Oxidative stress response: detection of superoxide radicals

We used nitroblue tetrazolium (NBT; N6876, Sigma-Aldrich) to detect superoxide radicals O_2^- presence (ROS), according to the method described by Rao and Davis [45]. Leaf fragments grown 2 days on phenanthrene concentrations of 0 and 400 µM (and even up to 800 µM phe) were immersed and infiltrated under vacuum with 3.5 $mg.ml^{-1}$ NBT staining solution in a potassium phosphate buffer (10 mM). Per treatment, we observed at least nine foliar portions from biological and technical triplicates. Then, samples were bathed in an acetic acid-glycerol-ethanol (in respective volumes 1:1:3) solution at 100°C for 5 min, before being bleached in 80% acetone.

NBT allowed the observation of O_2^- compounds which precipitate in blue color on plant tissues [34,46]. ROS production detected in leaf tissues reflects oxidative stress damages related to phenanthrene exposure. Leaves were then stored in a glycerol-ethanol solution (vol. 1:4) and photographed.

2.5. *In silico* and gene expression analysis

2.5.1. *In silico* search for candidate genes involved in phenanthrene stress response

Recently, xenomic candidates involved in PAH tolerance mechanisms were identified in *A. thaliana* grown in controlled conditions [35], and compared with functionally annotated crude oil responsive genes in *Spartina* [41]. Here, we investigated homologous genes in *Spartina* using the reference transcriptomes assembled from leaves and roots of *S. maritima* and *S. alterniflora* [47,48], in order to compare their expression profile in the parents and the allopolyploid under phenanthrene-induced stress in comparison to controlled conditions. Reference transcriptomes are composed of EST contigs resulting from assemblies of both short (Illumina) and long (Roche-454) reads from multiple cDNA libraries for each species (as described in [47,48]). Reads were assembled with 90% identity to build consensus sequences of homoeologs used as references that were functionally annotated. These transcriptomes resulted in 44,158 contigs in *S. alterniflora* and 60,644 contigs in *S. maritima*. To optimize the investigations, we also used genomic contigs assembled from short reads WGS (Whole Genome Shotgun) of *S. maritima* DNA libraries (A. Salmon & M. L. Ainouche, unpublished).

Based on the model described by Edwards *et al.* [38], we identified 99 differentially expressed (DE) candidate xenome genes (Supplemental Fig. S3, [35]). Because xenobiotic signaling and sensing mechanisms are still poorly understood, we focused on genes specifically involved in xenobiotic detoxification, conjugation, putative transformation and metabolization processes. These genes are classified within GSTs, GTs, CYPs, MTs, and ABC transporters. They represent 80 out of the total 99 DE genes reported in *Arabidopsis* under phenanthrene exposure (see [35]). We chose to select among them a set of overexpressed genes that might have a significant impact on the physiological plant tolerance to xenobiotics. Thus, we recovered 52 *A. thaliana* candidate genes (16 GSTs, 15 GTs, 15 CYPs, 1 MTs and 5 ABC transporters) for identifying their homologs in *Spartina* genomic and transcriptomic datasets.

In the present work, we aimed at identifying in *Spartina* the homologous xenome genes in *Arabidopsis* using full-length CDS sequences recovered from the TAIR database (TAIR10, http://www.arabidopsis.org). To improve our investigations, we also considered the rice genome (*Oryza sativa* 204, v7.0) available on Phytozome (http://phytozome.jgi.doe.gov). The pipeline

depicting step by step the investigation process of candidate genes in *Spartina* is summarized in Supplemental Fig. S4. We first identified some candidates already functionally annotated in the *Spartina* transcriptomes [47,49]. *O. sativa* homologs to *Arabidopsis* candidates were also identified using rice genome annotations. In addition, we performed BLAST alignments (BLASTn and tBLASTx) of *A. thaliana* gene sequences and their *O. sativa* homologs on *S. alterniflora* and *S. maritima* transcriptomes, and *S. maritima* genomic contigs. Gene hits with an e.value lower than 10^{-6} and homologies higher than 80% over at least 70 bases (BLASTn) or 50 bases (tBLASTx) were retained for *A. thaliana* and Monocot species alignments, while homologies higher than 80% over at least 100 bases (BLASTn) or 80 bases (tBLASTx) were retained for *O. sativa* - *Spartina* alignments.

2.5.2. GSTs phylogeny and gene expression analysis

Glutathione-S-transferases (GSTs) are a family of enzymes involved in many detoxification processes, including xenobiotic metabolism and limiting oxidative stress [50–53]. In the present work, the expression of GSTs genes were used as an example to highlight how the xenome components are transcriptionally regulated in the context of allopolyploidy under phenanthrene-induced stress.

- *GSTs phylogeny and homology assessment:*

We used GST homologs identified in *Spartina*, *Oryza*, and *Arabidopsis* as queries through BLASTp [54] requests on sorghum (*Sorghum bicolor* 313, v3.1), maize (*Zea mays* 284, v5b) and *Oropecium thomaeum* (386, v1.0) full length protein databases (from Phytozome) to identify putative orthologous sequences. *O. thomaeum* like *Spartina*, is member of the Chloridoideae subfamily, and currently represents the most related sequenced genome published to date. We retained homologies presenting an e.value cutoff lower than 10^{-6}, alignment lengths greater than 100 bases, and sequence identities of more than 60%.

To confirm candidate GSTs identified in *Spartina*, we validated the presence of functional protein domains by HMMsearch (Hidden Markov Models, e.value threshold 10^{-3}) against Pfam-A (version 30.0, [55]). We excised GST domains recovered in *Spartina* contigs, and aligned sequences using the MAFFT software (version 7 with basic parameters; [56]) on GST CDS sequences from *A. thaliana*, *O. sativa*, *S. bicolor*, *Z. mays* and *O. thomaeum.* We subjected the resulting alignment to Gblocks [57] to parse poorly aligned positions. Then, we performed phylogenetic analysis using the IQ-TREE web server [58]. We used the Maximum Likelihood method for tree construction with the TVM+G substitution model, and performed ultrafast

bootstrap analysis [59] on 10,000 replicates. We displayed phylogenetic tree using FigTree v1.4.3 (http://tree.bio.ed.ac.uk).

- *GSTs gene expression under phenanthrene-induced stress:*

We performed GST genes expression analysis on foliar fragments treated 10 days with phenanthrene concentrations of 0 and 400 µM. After sampling, we immediately froze leaves in liquid nitrogen. We proceeded to RNA extraction with Trizol reagent (Sigma), according to a protocol previously employed in *Spartina* [15,47]. This method consists in two successive cycles of precipitation, using isopropanol and absolute ethanol with sodium acetate (3M, pH= 5.3). We quantified each RNA sample using Nanodrop Spectrophotometer ND 1000 (Nanodrop Technologies, ThermoFisher Scientific Inc.) and purified extracts with a Turbo DNA-free kit (Ambion, Life technologies) to remove DNA contaminations, before storage at -80°C. We used about 700 ng of total RNA per sample for first-strand cDNA synthesis (kit ThermoScript RT-PCR, Invitrogen, Life technologies), and normalized cDNA concentrations to 5 $ng.\mu l^{-1}$ before RT-qPCR analysis.

Each amplified sample contained 0.5 ng of cDNA, 5 µl of PowerUp SYBR Green Master Mix (ThermoFisher), 1 µl of specific Reverse and Forward primers (5 µM), and sterile water for a final volume of 10 µl. We designed twenty base primers using Primer3 software (http://primer3.ut.ee/), with an expected amplicon size ranging between 100 and 200 bp, an average GC content of 55% and a Tm close to 60°C. We first tested primers on *Spartina* genomic DNA, and selected only single band amplifications for the quantification of gene expression.

In total, we analyzed the expression of 18 cDNA samples (3 species and 3 biological replicates from control and phe treated leaves) for each selected GST homologs (3 technical replicates were performed). We performed negative controls containing only sterile water, and 5 points dilution ranges with a pool of total cDNA (4 fold diluted steps from 0.5 to 2.10^{-3} $ng.\mu l^{-1}$) for each target gene. We conducted quantitative PCR on the LifeCycler 480 II (Roche), using the following program: pre-incubation at 95°C for 10 min, followed by 45 cycles of 10 sec incubation at 95°C, 10 sec annealing at 58°C, and 10 sec elongation at 68°C followed by optical reading. We performed melting curves (fluorescence acquisition every 0.5°C from 65 to 95°C) to check specificity of amplified fragments, and normalized levels of gene expression compared to the housekeeping gene glyceraldehyde-3-phosphate dehydrogenase (GA3PDH), which remains stable under these conditions [47,60]. This gene was amplified with the primer sequences AGAGTGCCTCGTCAAGGAGA (F) and CTCCCAAGCAATCCTCATGT (R).

2.6. Statistical analysis

We performed statistics with the RStudio software [61]. We analyzed phenanthrene quantification in foliar tissues between species, using one-way analysis of variance (ANOVA; model parameters checked by Shapiro and Bartlett tests), and pairwise comparisons using the Duncan procedure (at 95% confidence interval). We compared chlorophyll fluorescence data within species by Kruskal-Wallis multiple comparison's rank test with Bonferroni correction. We tested gene expression levels between species and treatments with two-way ANOVAs (model parameters checked by Shapiro and Bartlett tests), and conducted pairwise comparisons using *post hoc* Tukey HSD. We performed alternative analysis when model parameters were invalid, using Kruskal and Wallis and pairwise Wilcoxon-Mann Whitney tests. We also conducted comparisons between allopolyploid's expression levels and MPV (Mid-Parent Value, expected under additive parental gene expression in the allopolyploid) between treatments using the same procedure.

3. RESULTS

3.1. Phenanthrene absorption and histolocalisation

We observed histological sections of semi-thin treated (400 µM phe) and untreated leaves cultivated *in vitro* for one week by epifluorescence microscopy (Fig. 1). We did not detect phenanthrene bright spots (blue fluorescent patches) in control leaves (Fig. 1A). In treated leaves, we observed phenanthrene by specific blue fluorescence in specific tissues depending on the species considered, as indicated by orange arrows in Fig. 1B. We confirmed that phenanthrene presence in cells of the leaf margins and the xylem in the three *Spartina* species, but we also found xenobiotic in sclerenchyma cells in *S. alterniflora* and *S. anglica*. It was present in the mesophilic achlorophyllous parenchyma in the allopolyploid, and in the sub-epidermal parenchyma in *S. alterniflora*. If distinguishing phenanthrene fluorescence from lignin autofluorescence is challenging, because they emit at partially overlapping wavelengths (between 450 and 500 nm for lignin and 420-480 nm for phenanthrene on samples exited at 253 nm), phenanthrene specific emission spectra was detected at 420-440 nm which allowed to specifically identify the xenobiotic into the cellular matrix. In addition, more detailed analyses by confocal microscopy indicated that the presence of the pollutant is actually intracellular (see Fig. 1C), either cytosolic or vacuolar. These observations suggest that compartmentalization strategies could impact tolerance to xenobiotics of these three species.

We used GC-MS for phenanthrene quantification in order to estimate the free phenanthrene content absorbed by leaf tissues (Fig. 2). After 10 days treatment (100 µM phe), we found 213.8 ± 43.7 µg.gDW^{-1} phe in *S. anglica*, against 265.6 ± 65.1 in *S. alterniflora* and 468.8 ± 23.0 in *S. maritima*. These results revealed significantly higher phenanthrene content in *S. maritima* as compared to other species (p.value < 0.05). However, these data considered only phenanthrene in its toxic (and not chemically modified) form, which was not detected if subjected to any metabolic process (such as hydroxylation or glutathione conjugation).

3.2. Photosynthetic activity under phenanthrene-induced stress

After ten days of phenanthrene treatments (0, 100 and 400 µM phe), the average *Fv/Fm* ratios estimated on control leaves (0 µM phe) were about 0.80 ± 0.01 for *S. anglica* and 0.72 ± 0.03 for *S. alterniflora* and *S. maritima* (Fig. 3). In *S. anglica*, we did not observe any significant treatment impact, even under high phenanthrene concentrations (whether on 100 or 400 µM phe). However, the photosynthetic capacity of leaves was significantly reduced under 400 µM phe in *S. alterniflora* (*Fv*/*Fm* = 0.47 ± 0.06, p.value = 0.0113) and from 100 µM phe in *S. maritima* (*Fv*/*Fm* = 0.52 ± 0.08, p.value < 0.05).

3.3. Production of superoxide radicals under phenanthrene treatments

Under control conditions, NBT detection shows slight blue coloration whatever the considered species (Fig. 4). These colorations are highly localized, suggesting that superoxide radical production (ROS) occurred on specific locations, probably because of leaf handling. In both *S. alterniflora* and *S. anglica*, phenanthrene treatment up to 800 µM did not impact the production of superoxide radicals. In contrast, phenanthrene induced high oxidative stress on treated *S. maritima* leaves. This assumes that for such phenanthrene concentrations (whether 400 or 800 µM phe), oxidative stress was limited in *S. alterniflora* and *S. anglica* whereas *S. maritima* seems more sensitive showing a pronounced reaction. Interestingly, we found that long time exposure to phenanthrene treatment (30 days under 100 µM phe) did not induce any stress markers such as superoxide radical production and reduction of chlorophyll content in *S. anglica*. In contrast, the parental species *S. alterniflora* and *S. maritima* lost all chlorophyll contents and present severe senescent phenotype indicating cell death and tissue necrosis (results not shown).

3.4. Candidate genes involved in phenanthrene tolerance

In total, we validated 35 homologs in *S. maritima* and 31 in *S. alterniflora* using alignments to *A. thaliana* xenomic candidates. In complement, we added 11 homologies in *S. maritima* and 4 in *S.*

alterniflora using alignments to *O. sativa* candidates. Among this set of putative homologs, we used 12 candidate genes only characterized within *S. maritima* genomic contigs for a final BLAST request (BLASTn and tBLASTx) on the transcriptome of *S. alterniflora*, which revealed four additional homologies on this species. Finally, we identified sequence homologies for 46 and 39 xenome candidate genes in *S. maritima* and *S. alterniflora* respectively (see Supplemental Table S1), related to 47 *A. thaliana* locus (5 ABC transporters, 15 CYPs, 12 GSTs and 15 GTs). Among these genes, 38 present homologous sequences in both parental *Spartina* species.

In the present work, GSTs expression was used as an example to highlight how the xenome components are transcriptionally regulated in the context of the polyploidy under phenanthrene-induced stress. In total, we found 14 homologous sequences in the two parental *Spartina* species relative to 12 *A. thaliana*-GSTs. Phylogenetic reconstruction by Maximum Likelihood based on *A. thaliana*, rice, maize, sorghum and *O. thomaeum* GST CDS sequence alignments is displayed on Fig. 5 (TVM substitution model; [58]). We used rice and *Arabidopsis* GSTs from the *Omega* family as outgroup to root the tree. A total of 10 CDS sequences in *A. thaliana*, 14 in *O. sativa*, 19 in *S. bicolor*, 15 in *Z. mays*, 6 in *O. thomaeum* and 14 in *Spartina* were considered in the analysis. From this phylogenetic reconstruction, GST candidates retained in *Spartina* belong to the *Omega* GST gene family (Salt_2_contig34019, Salt_2_contig5351 and Smar_2_contig39931), and the plant specific *Tau* family. *Spartina* GST candidates were all similar to already known GSTs, and grouped within *Tau* or *Omega* GST families (ultrafast bootstrap value of 93). The tree topology distinguishes consistent specific clusters of *Poaceae* GSTs (highlighted in grey on the tree) as described by Jain *et al.* [62]. Among the 14 *Spartina* GST candidate sequences, we retained 6 contigs from *S. maritima* genomic sequencing after primer design (see Table 1, genes in bold on Supplemental Table S1) and followed their expressions patterns by RT-qPCR. However, we detected primer dimers on contig GA_02873 and removed the sequence from the analysis. Some of the technical replicates were invalidated and excluded from our analyses, but the limited extent of Cp (Crossing point) value distributions between them remain consistent. We checked PCR amplification efficiencies ($E= 10^{(-1/slope)}$) by standard curves, and relative gene expression values were calculated with the $2^{-\Delta Cp}$ method [63].

The relative expression ratios are presented in Fig. 6. *Spartina* GST homologous contigs identified present various expression patterns, depending on the species and the treatment applied. First, we compared expression profiles of GST contigs associated to *S. alterniflora*, *S. maritima*, and *S. anglica* within species between phenanthrene treatments (0 and 400 µM). In the parental species, the GST contigs selected did not display significant differential expressions considering the effect of ten days treatments on 400 µM phe. In the neo-allopolyploid, similar patterns were observed for

contigs GA_151485, GA_12349, GA_15763 and GA_263144. However, a significant down-regulation is detected in response to phenanthrene in *S. anglica* for the GA_47211 contig, where relative ratios (±SE) decreased from 1.93. 10^{-2} ± 3.53. 10^{-3} to 7.39. 10^{-3} ± 2.53. 10^{-3} (Fig. 6A, p.value < 0.01). Across species, additive expression patterns were observed in *S. anglica* for contigs GA_151485, GA_12349 and GA_15763, as MPV relative ratios estimated under control (0 µM phe) and treated conditions (400 µM phe) were respectively equivalent to those of the allopolyploid (p.value > 0.05). Conversely, we observed non-additive expressions in the allopolyploid for the contig GA_47211 with significant transgressive up-regulation (Fig. 6A, p.value < 0.001). We also observed that contig GA_263144 was expressed similarly to *S. maritima* in the allopolyploid under control condition (p.value = 0.50933). However, under stress condition its expression appeared slightly induced as compared to the same parent (Fig. 6E, p.value = 0.02809).

4. DISCUSSION

Understanding how plants adapt to challenging environment is a crucial question in evolutionary ecology. A growing body of evidence revealed the prominent role of whole genome duplication (polyploidy) in the plant diversification and adaptation [64]. In the present work, we explored the impact of allopolyploidization on plant xenobiotic tolerance in the saltmarsh lineage *Spartina* by comparing the recently formed allododecaploid species *S. anglica* to its parental species. This work represents the first comparative analyses performed to date between related *Spartina* species. The present analyses shed light on the detoxification processes involved in the three *Spartina* species exposed to phenanthrene in the context of natural allopolyploidization event, at the histochemical, biochemical and molecular levels.

4.1. Tolerance to phenanthrene-induced stress in *Spartina*

Phenanthrene histochemical investigations in *Spartina* revealed localized xenobiotic bright spots near the leaf margins, suggesting a potential establishment of evacuation processes by volatilization. Phenanthrene visualization in cells adjacent to the xylem tissues suggests that phenanthrene may be transported through the leaf by vascular elements as shown by Paterson *et al*. [65]. Furthermore, we confirmed by confocal microscopy that phenanthrene crossed the cell wall components and the plasmalemma, and was compartmented inside the cells (see Fig. 1C), either cytosolic or vacuolar. Intracellular presence of phenanthrene suggest that beyond being incorporated between cell walls, detoxification mechanisms of xenobiotics *via* metabolic pathways such as described in Edwards *et al.* [66] are ongoing in plant cells. However, differences observed

between *Spartina* species are introducing distinct cellular specific compartmentalization strategies, which may affect detoxifying properties. In *S. anglica* and *S. alterniflora*, we also detected phenanthrene in sclerenchyma and parenchyma, in contrast with *S. maritima* where it is only reported near the cells of the xylem. Highly localized phenanthrene bright spots suggest that xenobiotics in *S. alterniflora* and *S. anglica* were transferred into supportive and storage tissues, maybe for degradation and accumulation.

Concerning ROS production analyses, the absence of superoxide radicals observed in *S. anglica* and *S. alterniflora* even under high phenanthrene contents (800 µM phe) revealed high abilities of oxidative stress management. In contrast, Shiri *et al.* [34] recently analyzed the PAH sensitive species *Arabidopsis thaliana* and showed that ROS induction was detected at much lower phenanthrene concentrations (25 µM phe), supporting that phenanthrene stress levels used in our study highlights high tolerance abilities to PAHs in *Spartina* species.

4.2. Identification of homologous xenome genes in *Spartina*

Xenobiotic detoxification systems are still poorly understood in plants and have been explored in a few model systems [67,66]. Recent studies have explored the functional dynamics of the xenome in *Arabidopsis* under phenanthrene-induced stress [35,36,38], and comparisons with xenome responses to crude oil in natural *S. alterniflora* populations were performed [41]. Here, *in silico* detection of homologous xenome genes (as described in [35]) allowed an accurate identification of candidate genes involved in phenanthrene tolerance in *Spartina*. We retained a total of 38 genes from the *A. thaliana* xenome by homology searches in *Spartina*. Candidate xenome genes we identified represents putative phenanthrene detoxifying components in non-model Monocots such as *Spartina* which may be addressed in further analyses to study molecular mechanisms related to PAH detoxification.

We focused on the GST gene family which concentrate ubiquitous enzymes responsive to numerous stresses [51,52] to investigate the impact of allopolyploidization on xenome gene expression patterns under phenanthrene-induced stress. Several studies have demonstrated their role in the oxidative stress [68] by promoting antioxidant regeneration [69], or in xenobiotic detoxification by glutathione compounds conjugation [70]. Using available transcriptomic and genomic resources in the studied *Spartina* species [47,49] (A. Salmon & M. L. Ainouche, unpublished), we identified 14 *Spartina* GST contigs. Three of them (Salt_2_contig34019, Salt_2_contig5351 and Smar_2_contig39931) are grouped among the *Omega* GST family. Others belong to the plant specific GST *Tau* family, a class already described to have a major role in several detoxification processes [71].

Expression patterns of five GSTs from the *Tau* family were analyzed (filled triangles in the tree Fig. 5). Among four selected GST candidate genes, expression profiles did not reveal significant changes under phenanthrene-induced stress in the three *Spartina* species. However, significant down-regulation in response to phenanthrene found in *S. anglica* (contig GA_47211; Fig. 6A) illustrates divergent regulation pathways opportunities under genome duplication event. While most of GST candidate genes analyzed did not present significant responses to phenanthrene, it is not clear how these genes may be involved in detoxification response to phenanthrene in *Spartina*, as suggested by Alvarez *et al.* [41]. However, *Spartina* and *Arabidopsis* belong to divergent lineages in Monocots and Eudicots respectively, which separated 170-220 MYA [72]. Thus, tolerance to organic xenobiotics may then involve distinct metabolic pathways and detoxification mechanisms, maybe through different transformation processes (Supplemental Fig. S3) recruiting other GSTs, GTs and malonyltransferases [36,66]. Interestingly, our phylogenetic analysis revealed Poaceae specific GST clades, as described by Jain *et al.* [62]. Hence, such genes may have acquired novel functions, as illustrated by the GST *Spartina* contigs which appeared quite distant from other GSTs in the phylogenetic analysis (see Fig. 5). Here, we only focused on GSTs as an example, but larger xenome profiling between species in controlled conditions are needed to clarify molecular mechanisms involved in phenanthrene detoxification in *Spartina*.

4.3. Does allopolyploidy impact tolerance to xenobiotics?

The recent formation of *S. anglica* during the end of the 19th century offers a unique opportunity to explore the early evolutionary changes associated with the formation of a new allopolyploid species in natural populations, comparing the neo-allopolyploid to its parental species [12]. Morphological and ecological traits of the rapidly expanding neo-allopolyploid compared to its parental species have been thoroughly described [73,74].

Our comparative physiological analysis highlights that *S. maritima* is the most sensitive species to PAH-induced stress. The significant production of superoxide radicals in *S. maritima* leaves indicates that oxidative stress through superoxide production was pronounced in this species, contrasting with the tolerance exhibited by *S. alterniflora* and *S. anglica*, which developed stress tolerance abilities (Figure 2 and 4). *Spartina maritima* has reduced antioxidant scavenging capacities, thus increasing phenanthrene toxicity. Our findings also agree with the reduction in photosynthetic activity observed in *S. maritima*, as ROS are known to negatively impact photosynthetic rates [75]. Moreover, phenanthrene uptake assays performed in leaf tissues revealed contrasted free phenanthrene contents among species, the lowest amount being quantified in the neo-allopolyploid *S. anglica* and the highest in *S. maritima*. In complement, additional

histolocalisation of xenobiotics into *S. alterniflora* and *S. anglica* plant tissues (sclerenchyma and parenchyma) may be related with enhanced detoxification mechanisms.

Hence, we provide experimental data supporting that enhanced xenobiotic tolerance are found in *S. anglica* and *S. alterniflora* in contrast with pronounced sensitivity in *S. maritima*, consistently with *Fv/Fm* ratio measured under 100 µM phe, significantly reduced in the paternal parent in contrast to other species. Altogether, these findings may be related to ecological traits of the compared species. *S. anglica* and *S. alterniflora* are described as vigorous invasive species [76–81] whereas *S. maritima* is restricted to its native area along European and African coast where its seems declining in some sites (*e.g.* England; [82]). The three species usually colonize low mash habitats and mudflats with lower salinity ranges [83–85] but *S. anglica* and *S. alterniflora* are also present in areas more frequently flooded or high marsh zones, and may be exposed to stronger salt and drought levels [77,86–88].

The photosynthetic system is a key indicator to estimate plant tolerance to biotic and abiotic stress. Previous studies showed that *S. alterniflora* photosynthetic rates were severely affected when growing in PAH contaminated soils [89,90]. Our study reveals that phenanthrene stress tolerance increased with ploidy level in *Spartina*, since *S. anglica* maintained high chlorophyll fluorescence levels under phenanthrene-induced stress in contrast to its parental species. Under phenanthrene treatment, we found that photosynthetic activity was significantly reduced in the parental species. Thus, it seems that such phenanthrene concentrations (400 µM phe) did not affect *S. anglica* photosynthetic apparatus, as opposed to the parental species. Moreover, by comparing *S. anglica* to *S. alterniflora* we observed different patterns of phenanthrene localization, mainly accumulated in the sub-epidermal parenchyma in *S. alterniflora*, in contrast to the mesophilic parenchyma in *S. anglica*.

Differences in tolerance levels between species were detected through enhanced tolerance reported in *S. anglica*, compared to its parental species (Figure 1 and 3), consistently with long term tolerance experiments (30 days under 100 µM phe) which highlight senescent phenotypes in the parental species while *S. anglica* did not exhibit any phenotypic stress markers. This suggests that the allopolyploid *S. anglica* cope with chronic organic xenobiotic exposure through efficient metabolic detoxification pathways. As the recent origin and the low inter-individual genetic diversity related to clonal propagation reported in *S. anglica* are limiting the effects of selection acting on different genotypes [9–11], it is reasonable to speculate that tolerance to PAHs results from immediate evolutionary effects of WGD. To our knowledge, the present work demonstrates

for the first time that allopolyploidy may enhance tolerance to organic pollutants. Nevertheless, one can keep in mind that other mechanisms resulting from the species history might interact.

Allopolyploidy highly impacts gene expression (*i.e.* deviation from expected parental additivity), and may have critical adaptive impact on newly formed polyploid species [91]. Previous transcriptomic investigations in polyploid *Spartina* were performed in both controlled [15] and natural [92] conditions and revealed various expression patterns in *S. anglica* compared to its parental species. In the present study, expression of the GST genes involved in *A. thaliana* xenobiotic tolerance was explored. Transgressive up-regulation was recorded for contig GA_47211 with respect to MPV and parental expression patterns. Non-additive expression was also exhibited by the contig GA_263144 in control condition, while expression in *S. anglica* was statistically equivalent to its expression in *S. maritima*, but differed from the MPV and from its expression in *S. alterniflora* (expression dominance mimicking the paternal expression pattern). Interestingly, paternal dominance appeared to be lost under stress conditions, as expression in *S. anglica* was higher and additive with respect to parental expression patterns (statistically equivalent to the MPV).

Allopolyploidy is a combination of two different evolutionary events, *i.e.* the merger of divergent genomes (resulting from hybridization) and whole genome duplication (resulting from polyploidy) that shape the newly formed allopolyploid genome [13,15]. Thus, changes detected in *S. anglica* may reflect one or both evolutionary events. Additional comparative analyses of the xenome in the F1 hybrid (*S. x townsendii*) will help deciphering the relative contributions of hybridization and/or genome doubling *per se*. Expression plasticity exploiting the union of divergent expression and regulatory networks inherited from *S. maritima* and *S. alterniflora* which diverged since 2-4 MYA [93], combined with important epigenetic alterations [13,14], most likely represent a key component in *S. anglica* enhanced tolerance to xenobiotics. As halophytes represent an emerging trend in phytoremediation [94], our results are supporting using *S. anglica* for such purpose on organic pollutants.

Author contributions

A.E, A.S and M.A. designed the experiments. A.E., O.L. and A.C.R. performed the experiments. A.E., A.S., M.A. and A.C.R. analyzed data. A.E., A.S., M.A. and A.C.R. wrote the article.

Acknowledgements

This work was supported by the Ministère de l'Enseignement Supérieur et de la Recherche, by the CNRS, and the Observatoire des Sciences et de l'Univers de Rennes (OSUR). The authors would

like to knowledge Olivier Catrice with his assistance for the achievement of confocal microscopy analysis. We also thank two anonymous reviewers for their constructive comments.

Conflicts of interest: ‘none'

REFERENCES

[1] D.E. Soltis, V.A. Albert, J. Leebens-Mack, C.D. Bell, A.H. Paterson, C. Zheng, D. Sankoff, C.W. de Pamphilis, P.K. Wall, P.S. Soltis, Polyploidy and angiosperm diversification, Am. J. Bot. 96 (2009) 336–348.

[2] L. Comai, The advantages and disadvantages of being polyploid, Nat. Rev. Genet. 6 (2005) 836–846.

[3] A. Madlung, J.F. Wendel, Genetic and epigenetic aspects of polyploid evolution in plants, Cytogenet. Genome Res. 140 (2013) 270–285.

[4] P.S. Soltis, D.B. Marchant, Y. Van de Peer, D.E. Soltis, Polyploidy and genome evolution in plants, Curr. Opin. Genet. Dev. 35 (2015) 119–125.

[5] K. Alix, P.R. Gérard, T. Schwarzacher, J.S. (Pat) Heslop-Harrison, Polyploidy and interspecific hybridization: partners for adaptation, speciation and evolution in plants, Ann. Bot. 120 (2017) 183–194.

[6] J.J. Doyle, L.E. Flagel, A.H. Paterson, R.A. Rapp, D.E. Soltis, P.S. Soltis, J.F. Wendel, Evolutionary genetics of genome merger and doubling in plants, Annu. Rev. Genet. 42 (2008) 443–461.

[7] P.M. Peterson, K. Romaschenko, Y.H. Arrieta, J.M. Saarela, A molecular phylogeny and new subgeneric classification of *Sporobolus*; (Poaceae: Chloridoideae: Sporobolinae), Taxon. 63 (2014) 1212–1243.

[8] S. Lowe, M. Browne, S. Boudjelas, M. De Poorter, 100 of the world's worst invasive alien species: A selection from the Global invasive species database., Invasive Species Spec. Group ISSG Spec. Group Species Surviv. Comm. SSC World Conserv. Union IUCN. First published as special lift-out in Aliens 12 (2000) 12pp.

[9] M.L. Ainouche, A. Baumel, A. Salmon, G. Yannic, Hybridization, polyploidy and speciation in *Spartina* (Poaceae), New Phytol. 161 (2003) 165–172.

[10] M. Ainouche, H. Chelaifa, J. Ferreira, S. Bellot, A. Ainouche, A. Salmon, Polyploid evolution in *Spartina*: Dealing with highly redundant hybrid genomes, in: P.S. Soltis, D.E. Soltis (Eds.), Polyploidy Genome Evol., Springer Berlin Heidelberg, Berlin, Heidelberg, 2012: pp. 225–243.

[11] A. Baumel, M.L. Ainouche, J.E. Levasseur, Molecular investigations in populations of *Spartina anglica* C.E. Hubbard (Poaceae) invading coastal Brittany (France), Mol. Ecol. 10 (2001) 1689–1701.

[12] M.L. Ainouche, A. Baumel, A. Salmon, *Spartina anglica* C. E. Hubbard: a natural model system for analysing early evolutionary changes that affect allopolyploid genomes: evolution of the *Spartina anglica*, Biol. J. Linn. Soc. 82 (2004) 475–484.

[13] A. Salmon, M.L. Ainouche, J.F. Wendel, Genetic and epigenetic consequences of recent hybridization and polyploidy in *Spartina* (Poaceae), Mol. Ecol. 14 (2005) 1163–1175.

[14] C. Parisod, A. Salmon, T. Zerjal, M. Tenaillon, M.-A. Grandbastien, M. Ainouche, Rapid structural and epigenetic reorganization near transposable elements in hybrid and allopolyploid genomes in *Spartina*, New Phytol. 184 (2009) 1003–1015.

[15] H. Chelaifa, A. Monnier, M. Ainouche, Transcriptomic changes following recent natural hybridization and allopolyploidy in the salt marsh species *Spartina* × *townsendii* and *Spartina anglica* (Poaceae), New Phytol. 186 (2010) 161–174.

[16] B.R. Maricle, R.W. Lee, Aerenchyma development and oxygen transport in the estuarine cordgrasses *Spartina alterniflora* and *S. anglica*, Aquat. Bot. 74 (2002) 109–120.

[17] B.R. Maricle, J.J. Crosier, B.C. Bussiere, R.W. Lee, Respiratory enzyme activities correlate with anoxia tolerance in salt marsh grasses, J. Exp. Mar. Biol. Ecol. 337 (2006) 30–37.

[18] J.B. Adams, G.C. Bate, Ecological implications of tolerance of salinity and inundation by *Spartina maritima*, Aquat. Bot. 52 (1995) 183–191.

[19] A.W. Watts, T.P. Ballestero, K.H. Gardner, Uptake of polycyclic aromatic hydrocarbons (PAHs) in salt marsh plants *Spartina alterniflora* grown in contaminated sediments, Chemosphere. 62 (2006) 1253–1260.

[20] I.A. Mendelssohn, G.L. Andersen, L.P. Rozas, Oil impacts on coastal wetlands: Implications for the Mississippi river delta ecosystem after the deepwater horizon oil spill, BioScience. 62 (2012) 562–574.

[21] S. Redondo-Gomez, Bioaccumulation of heavy metals in *Spartina*, Funct. Plant Biol. (2013).

[22] G. Curado, A.E. Rubio-Casal, E. Figueroa, J.M. Castillo, Potential of *Spartina maritima* in restored salt marshes for phytoremediation of metals in a highly polluted estuary, Int. J. Phytoremediation. 16 (2014) 1209–1220.

[23] P. Biber, W. Wu, M. Peterson, Z. Liu, L. Pham, Oil contamination in Mississippi salt marsh habitats and the impacts to *Spartina alterniflora* photosynthesis, in: J. Alford, M. Peterson, C. Green (Eds.), Impacts Oil Spill Disasters Mar. Habitats Fish. N. Am., CRC Press, 2014: pp. 133–172.

[24] A. Bergen, C. Alderson, R. Bergfors, C. Aquila, M.A. Matsil, Restoration of a Spartina alterniflorasalt marsh following a fuel oil spill, New York City, NY, Wetl. Ecol. Manag. 8 (2000) 185–195. doi:10.1023/A:1008496519697.

[25] C.H. Chaîneau, J.L. Morel, J. Oudot, Phytotoxicity and plant uptake of fuel oil hydrocarbons, J. Environ. Qual. 26 (1997) 1478.

[26] P.J. Harvey, B.F. Campanella, P.M.L. Castro, H. Harms, E. Lichtfouse, A.R. Schäffner, S. Smrcek, D. Werck-Reichhart, Phytoremediation of polyaromatic hydrocarbons, anilines and phenols, Environ. Sci. Pollut. Res. 9 (2002) 29–47.

[27] B.M. Greenberg, PAH Interactions with plants: Uptake, toxicity and phytoremediation, in: P.E.T. Douben (Ed.), PAHs Ecotoxicological Perspect., John Wiley & Sons, Ltd, 2003: pp. 263–273.

[28] Y. Gao, L. Zhu, Plant uptake, accumulation and translocation of phenanthrene and pyrene in soils, Chemosphere. 55 (2004) 1169–1178.

[29] E. Pilon-Smits, Phytoremediation, Annu. Rev. Plant Biol. 56 (2005) 15–39.

[30] X. Zhan, X. Zhang, X. Yin, H. Ma, J. Liang, L. Zhou, T. Jiang, G. Xu, H+/phenanthrene symporter and aquaglyceroporin are implicated in phenanthrene uptake by wheat (L.) roots, J. Environ. Qual. 41 (2012) 188.

[31] M. Alkio, T.M. Tabuchi, X. Wang, A. Colon-Carmona, Stress responses to polycyclic aromatic hydrocarbons in *Arabidopsis* include growth inhibition and hypersensitive response-like symptoms, J. Exp. Bot. 56 (2005) 2983–2994.

[32] H. Liu, D. Weisman, Y. Ye, B. Cui, Y. Huang, A. Colón-Carmona, Z. Wang, An oxidative stress response to polycyclic aromatic hydrocarbon exposure is rapid and complex in *Arabidopsis thaliana*, Plant Sci. 176 (2009) 375–382.

[33] C. Sulmon, G. Gouesbet, F. Ramel, F. Cabello-Hurtado, C. Penno, N. Bechtold, I. Couée, A.E. Amrani, Carbon dynamics, development and stress responses in *Arabidopsis*: Involvement of the APL4 subunit of ADP-Glucose pyrophosphorylase (starch synthesis), PLoS ONE. 6 (2011).

[34] M. Shiri, M. Rabhi, C. Abdelly, A.E. Amrani, The halophytic model plant *Thellungiella salsuginea* exhibited increased tolerance to phenanthrene-induced stress in comparison with the glycophitic one *Arabidopsis thaliana*: Application for phytoremediation, Ecol. Eng. 74 (2015) 125–134.

[35] A.-S. Dumas, L. Taconnat, E. Barbas, G. Rigaill, O. Catrice, D. Bernard, A. Benamar, D. Macherel, A. El Amrani, R. Berthomé, Unraveling the early molecular and physiological mechanisms involved in response to phenanthrene exposure, BMC Genomics. 17 (2016).

[36] D. Weisman, M. Alkio, A. Colón-Carmona, Transcriptional responses to polycyclic aromatic hydrocarbon-induced stress in *Arabidopsis thaliana* reveal the involvement of hormone and defense signaling pathways, BMC Plant Biol. 10 (2010) 59.

[37] A.C. Singer, D.E. Crowley, I.P. Thompson, Secondary plant metabolites in phytoremediation and biotransformation, Trends Biotechnol. 21 (2003) 123–130.

[38] R. Edwards, D.P. Dixon, I. Cummins, M. Brazier-Hicks, M. Skipsey, New perspectives on the metabolism and detoxification of synthetic compounds in plants, in: P. Schröder, C.D. Collins (Eds.), Org. Xenobiotics Plants, Springer Netherlands, Dordrecht, 2011: pp. 125–148.

[39] G. Taguchi, T. Ubukata, H. Nozue, Y. Kobayashi, M. Takahi, H. Yamamoto, N. Hayashida, Malonylation is a key reaction in the metabolism of xenobiotic phenolic glucosides in *Arabidopsis* and tobacco: Phenolic-xenobiotics metabolism in Arabidopsis, Plant J. 63 (2010) 1031–1041.

[40] A. El Amrani, A.-S. Dumas, L.Y. Wick, E. Yergeau, R. Berthomé, "Omics" Insights into PAH Degradation Toward Improved Green Remediation Biotechnologies, Environ. Sci. Technol. 49 (2015) 11281–11291.

[41] M. Alvarez, J. Ferreira de Carvalho, A. Salmon, M.L. Ainouche, A. Cavé-Radet, A. El Amrani, T.E. Foster, S. Moyer, C.L. Richards, Transcriptome response to the *Deepwater Horizon* oil spill identifies novel candidate genes for oil tolerance in natural populations of the foundation plant *Spartina alterniflora*, Mol. Ecol. (2018).

[42] Z. Liu, J. Liu, Q. Zhu, W. Wu, The weathering of oil after the *Deepwater Horizon* oil spill: insights from the chemical composition of the oil from the sea surface, salt marshes and sediments, Environ. Res. Lett. 7 (2012) 035302.

[43] K.E.C. Smith, K.C. Jones, Particles and vegetation: implications for the transfer of particle-bound organic contaminants to vegetation, Sci. Total Environ. 246 (2000) 207–236.

[44] A. Narayan, M. Misra, R. Singh, Chlorophyll fluorescence in plant biology, in: P.D.A.N. Misra (Ed.), Biophysics, InTech, 2012.

[45] M.V. Rao, K.R. Davis, Ozone-induced cell death occurs via two distinct mechanisms in *Arabidopsis*: the role of salicylic acid, Plant J. 17 (1999) 603–614.

[46] F. Ramel, C. Sulmon, F. Cabello-Hurtado, L. Taconnat, M.-L. Martin-Magniette, J.-P. Renou, A. El Amrani, I. Couée, G. Gouesbet, Genome-wide interacting effects of sucrose and herbicide-mediated stress in *Arabidopsis thaliana*: novel insights into atrazine toxicity and sucrose-induced tolerance, BMC Genomics. 8 (2007) 450.

[47] J. Ferreira de Carvalho, J. Poulain, C. Da Silva, P. Wincker, S. Michon-Coudouel, A. Dheilly, D. Naquin, J. Boutte, A. Salmon, M. Ainouche, Transcriptome de novo assembly from next-generation sequencing and comparative analyses in the hexaploid salt marsh species *Spartina maritima* and *Spartina alterniflora* (Poaceae), Heredity. 110 (2013) 181–193.

[48] J. Boutte, B. Aliaga, O. Lima, J. Ferreira de Carvalho, A. Ainouche, J. Macas, M. Rousseau-Gueutin, O. Coriton, M. Ainouche, A. Salmon, Haplotype detection from Next Generation Sequencing in high ploidy-level species: 45S rDNA gene copies in the hexaploid *Spartina maritima*, G3 GenesGenomesGenetics. (2015).

[49] J. Boutte, C.J. Ferreira de, M. Rousseau-Gueutin, J. Poulain, C. Da Silva, P. Wincker, M. Ainouche, A. Salmon, Reference transcriptomes and detection of duplicated copies in hexaploid and allododecaploid *Spartina* species (Poaceae), Genome Biol. Evol. (2016) evw209.

[50] A.S. Milligan, A. Daly, M.A.J. Parry, P. Lazzeri, I. Jepson, The expression of a maize glutathione S-transferase gene in transgenic wheat confers herbicide tolerance, both in planta and *in vitro*, Mol. Breed. 7 (2001) 301–315.

[51] N.E. Labrou, A.C. Papageorgiou, O. Pavli, E. Flemetakis, Plant GSTome: structure and functional role in xenome network and plant stress response, Curr. Opin. Biotechnol. 32 (2015) 186–194.

[52] K. Nahar, M. Hasanuzzaman, M. Fujita, Physiological roles of glutathione in conferring abiotic stress tolerance to plants, in: N. Tuteja, S.S. Gill (Eds.), Abiotic Stress Response Plants, Wiley-VCH Verlag GmbH & Co. KGaA, Weinheim, Germany, 2016: pp. 155–184.

[53] B.P. DeRidder, Induction of Glutathione S-Transferases in *Arabidopsis* by herbicide safeners, PLANT Physiol. 130 (2002) 1497–1505.

[54] S.F. Altschul, W. Gish, W. Miller, E.W. Myers, D.J. Lipman, Basic local alignment search tool, J. Mol. Biol. 215 (1990) 403–410.

[55] R.D. Finn, P. Coggill, R.Y. Eberhardt, S.R. Eddy, J. Mistry, A.L. Mitchell, S.C. Potter, M. Punta, M. Qureshi, A. Sangrador-Vegas, G.A. Salazar, J. Tate, A. Bateman, The Pfam protein families database: towards a more sustainable future, Nucleic Acids Res. 44 (2016) D279–D285.

[56] K. Katoh, D.M. Standley, MAFFT Multiple sequence alignment software version 7: Improvements in performance and usability, Mol. Biol. Evol. 30 (2013) 772–780.

[57] G. Talavera, J. Castresana, K. Kjer, R. Page, J. Sullivan, Improvement of phylogenies after removing divergent and ambiguously aligned blocks from protein sequence alignments, Syst. Biol. 56 (2007) 564–577.

[58] L.-T. Nguyen, H.A. Schmidt, A. von Haeseler, B.Q. Minh, IQ-TREE: A Fast and Effective Stochastic Algorithm for Estimating Maximum-Likelihood Phylogenies, Mol. Biol. Evol. 32 (2015) 268–274.

[59] B.Q. Minh, M.A.T. Nguyen, A. von Haeseler, Ultrafast Approximation for Phylogenetic Bootstrap, Mol. Biol. Evol. 30 (2013) 1188–1195.

[60] N. Baisakh, P.K. Subudhi, N.P. Parami, cDNA-AFLP analysis reveals differential gene expression in response to salt stress in a halophyte *Spartina alterniflora* Loisel, Plant Sci. 170 (2006) 1141–1149.

[61] R Core Team, R: a language and environement for statistical computing, R foundation for statistical computing, Vienne (Autriche), 2015. http://www.R-project.org/.

[62] M. Jain, C. Ghanashyam, A. Bhattacharjee, Comprehensive expression analysis suggests overlapping and specific roles of rice glutathione S-transferase genes during development and stress responses, BMC Genomics. 11 (2010) 73.

[63] M.W. Pfaffl, A new mathematical model for relative quantification in real-time RT-PCR, Nucleic Acids Res. 29 (2001) 45.

[64] Y. Van de Peer, E. Mizrachi, K. Marchal, The evolutionary significance of polyploidy, Nat. Rev. Genet. 18 (2017) 411–424.

[65] S. Paterson, D. Mackay, C. McFarlane, A model of organic chemical uptake by plants from soil and the atmosphere, Environ. Sci. Technol. 28 (1994) 2259–2266.

[66] R. Edwards, M. Brazier-Hicks, D.P. Dixon, I. Cummins, Chemical manipulation of antioxidant defences in plants, in: Adv. Bot. Res., Elsevier, 2005: pp. 1–32.

[67] H. Sandermann, Plant metabolism of xenobiotics, Trends Biochem. Sci. 17 (1992) 82–84.

[68] P.G. Sappl, A.J. Carroll, R. Clifton, R. Lister, J. Whelan, A. Harvey Millar, K.B. Singh, The *Arabidopsis* glutathione transferase gene family displays complex stress regulation and co-silencing multiple genes results in altered metabolic sensitivity to oxidative stress: Genomic and reverse genetic analysis of plant GSTs, Plant J. 58 (2009) 53–68.

[69] P.-A. Lallement, B. Brouwer, O. Keech, A. Hecker, N. Rouhier, The still mysterious roles of cysteine-containing glutathione transferases in plants, Front. Pharmacol. 5 (2014).

[70] D.P. Dixon, R. Edwards, Glutathione Transferases, Arab. Book. 8 (2010).

[71] D.P. Dixon, B.G. Davis, R. Edwards, Functional Divergence in the Glutathione transferase superfamily in plants. Identification of two classes with putative functions in redox homeostasis in *Arabidopsis thaliana*, J. Biol. Chem. 277 (2002) 30859–30869.

[72] Y.-W. Yang, K.-N. Lai, P.-Y. Tai, W.-H. Li, Rates of nucleotide substitution in angiosperm mitochondrial DNA sequences and dates of divergence between *Brassica* and other angiosperm lineages, J. Mol. Evol. 48 (1999) 597–604.

[73] C.J. Marchant, Evolution in *Spartina* (Gramineae): I. The history and morphology of the genus in Britain, J. Linn. Soc. Lond. Bot. 60 (1967) 1–24.

[74] A.J. Gray, D.F. Marshall, A.F. Raybould, A Century of Evolution in *Spartina anglica*, in: Adv. Ecol. Res., Elsevier, 1991: pp. 1–62.

[75] A.R. Reddy, A.S. Raghavendra, Photooxidative stress, in: K.. Madhava Rao, A.S. Raghavendra, K. Janardhan Reddy (Eds.), Physiol. Mol. Biol. Stress Toler. Plants, Kluwer Academic Publishers, Dordrecht, 2006: pp. 157–186.

[76] Q. Wang, S.-Q. An, Z.-J. Ma, J.-K. Chen, B. Li, Invasive *Spartina alterniflora*: biology, ecology and management, Acta Phytotaxon. Sin. 44 (2006) 559.

[77] C.M. Anderson, M. Treshow, A Review of Environmental and Genetic Factors That Affect Height in *Spartina alterniflora* Loisel. (Salt Marsh Cord Grass), Estuaries. 3 (1980) 168.

[78] J.D. Thompson, The biology of an invasive plant, 41 (1991) 393–401.

[79] J. Adams, E. van Wyk, T. Riddin, First record of *Spartina alterniflora* in southern Africa indicates adaptive potential of this saline grass, Biol. Invasions. 18 (2016) 2153–2158.

[80] M. Ainouche, A. Gray, Invasive *Spartina*: lessons and challenges, Biol. Invasions. 18 (2016) 2119–2122.

[81] W.H. Elmer, R.E. Marra, H. Li, B. Li, Incidence of *Fusarium spp.* on the invasive *Spartina alterniflora* on Chongming Island, Shanghai, China, Biol. Invasions. 18 (2016) 2221–2227.

[82] A.F. Raybould, A.J. Gray, M.J. Lawrence, D.F. Marshall, The evolution of *Spartina anglica* C. E. Hubbard (Gramineae): genetic variation and status of the parental species in Britain, Biol. J. Linn. Soc. 44 (1991) 369–380.

[83] M.D. Bertness, Zonation of *Spartina patens* and *Spartina alterniflora* in New England salt marsh, Ecology. 72 (1991) 138.

[84] J.M. Castillo, L. Fernandez-Baco, E.M. Castellanos, C.J. Luque, M.E. FigUeroa, A.J. Davy, Lower limits of *Spartina densiflora* and *S. maritima* in a Mediterranean salt marsh determined by different ecophysiological tolerances, J. Ecol. 88 (2000) 801–812.

[85] S.D. Hacker, D. Heimer, M.N. Dethier, A marine plant (*Spartina anglica*) invades widely varying habitats: Potential mechanisms of invasion and control, Biol. Invasions. 3 (2001) 211–217.

[86] C.L. Richards, S.C. Pennings, L.A. Donovan, Habitat range and phenotypic variation in salt marsh plants, Plant Ecol. 176 (2005) 263–273.

[87] C.L. Richards, J.L. Hamrick, L.A. Donovan, R. Mauricio, Unexpectedly high clonal diversity of two salt marsh perennials across a severe environmental gradient, Ecol. Lett. 7 (2004) 1155–1162.

[88] J. Rozema, H. Gude, G. Pollak, An ecophysiological study of the salt secretion of four halophytes, New Phytol. 89 (1981) 201–217.

[89] S.R. Pezeshki, R.D. De Laune, Effect of crude oil on gas exchange functions of *Juncus roemerianus* and *Spartina alterniflora*, Water. Air. Soil Pollut. 68 (1993) 461–468.

[90] Q. Lin, I.A. Mendelssohn, Evaluation of tolerance limits for restauration anf phytoremediation with *Spartina alterniflora* in crude oil contaminated coastal salt marshes, Int. Oil Spill Conf. Proc. 2008 (2008) 869–873.

[91] M.L. Ainouche, J.F. Wendel, Polyploid speciation and genome evolution: Lessons from recent allopolyploids, in: P. Pontarotti (Ed.), Evol. Biol. Genome Evol. Speciat. Coevol. Orig. Life, Springer International Publishing, Cham, 2014: pp. 87–113.

[92] J. Ferreira de Carvalho, J. Boutte, P. Bourdaud, H. Chelaifa, K. Ainouche, A. Salmon, M. Ainouche, Gene expression variation in natural populations of hexaploid and allododecaploid *Spartina* species (Poaceae), Plant Syst. Evol. (2017).

[93] M. Rousseau-Gueutin, S. Bellot, G.E. Martin, J. Boutte, H. Chelaifa, O. Lima, S. Michon-Coudouel, D. Naquin, A. Salmon, K. Ainouche, M. Ainouche, The chloroplast genome of the

hexaploid *Spartina maritima* (Poaceae, Chloridoideae): Comparative analyses and molecular dating, Mol. Phylogenet. Evol. 93 (2015) 5–16.

[94] E. Manousaki, N. Kalogerakis, Halophytes—An Emerging Trend in Phytoremediation, Int. J. Phytoremediation. 13 (2011) 959–969.

[95] W.S. Alves, E.A. Manoel, N.S. Santos, R.O. Nunes, G.C. Domiciano, M.R. Soares, Detection of polycyclic aromatic hydrocarbons (PAHs) in Medicago sativa L. by fluorescence microscopy, Micron. 95 (2017) 23–30.

FIGURES AND TABLES

Figure 1. Histological observation of cross sections of *Spartina* leaves by confocal and epifluorescence microscopy. A: Phe accumulated in the cells was detected by specific blue fluorescent bright spots. In control leaves, no phe specific fluorescence was observed (scale bars= 50 µm). B: Phe locations are different between species treated with 400 µM phe (scale bars= 100 µm). In the three species, phe was detected in the neighboring cells of the xylem. Phe was also specifically found in the sclerenchyma cells close to leaf margins, and in the mesophilic achlorophyllous parenchyma in *S. anglica*. In *S. alterniflora*, it is also present in the parenchyma cells and the sub-epidermal sclerenchyma. C: Phenanthrene colocalization into *Spartina* leaf plant tissues by confocal microscopy (scale bar = 25 µm.). Detection of the phenanthrene specific emission spectrum allowed us to identify the pollutant by assigning it a violet coloration. Confocal microscopy pics clearly distinguish phenanthrene (1) intracellular presence inside the cell walls (2), and chlorophyll fluorescence in red (3).

Figure 2. Phe concentrations in *Spartina* leaves cultivated 10 days on medium containing 100 µM phe. Means are calculated from three biological replicates; bars correspond to standard errors. The different letters are corresponding to significant concentration differences according to Duncan's test (p.value < 0.05).

Figure 3. *Fv/Fm* ratio under phenanthrene treatment (0, 100 and 400 µM), an index of the maximum quantum yield of PS II for each of the three species of *Spartina*. Measurements were carried out after 10 days of phe treatment. Means are calculated from three biological replicates; bars correspond to the standard errors. Values annotated with different letters by species are significantly different according to Kruskal-Wallis multiple comparison's test (with Bonferroni correction, p.value < 0.05).

Figure 4. Visualization of superoxide radical production upon leaves NBT infiltrations. *Spartina* leaves were cultivated 2 days in medium containing 0, 400 and up to 800 µM phe. Superoxide radicals were detected by the presence of blue spots. Light blue spots were visible on *S. anglica* and *S. alterniflora* leaves, whatever the treatment provided. In contrast, *S. maritima* leaves present a severe coloration from 400 µM phe, reflecting a strong oxidative stress. Scale bars = 1.5 mm.

Figure 5. GSTs phylogenetic reconstruction by Maximum Likelihood method based on the TVM (transversion) substitution model with a discrete Gamma distribution (4 categories). In total, 78 CDS sequences were considered among *A. thaliana*, *O. sativa*, *S. bicolor*, *Z. mays*, *O. thomaeum* and *Spartina*. Tree is rooted by CDS sequences from the *Omega* GST gene family, and numbers at the nodes represent ultrafast bootstrap values from 10,000 replicates. *Spartina* contigs are displayed with black triangles, those we evaluate their expression by RT-qPCR are stained and belong to the *Tau* family. Corresponding sequences IDs: GRMZM─ for *Z. mays*; Sobic─ for *S. bicolor*; Oropecium─ for *O. thomaeum*. Scale bar indicates 0.1 residue substitution per site.

Figure 6. Relative expression levels of five candidates contigs (GST homologs) estimated by RT-qPCR on three biological and technical replicates for each *Spartina* species in control conditions and under phenanthrene induced stress (0 and 400 µM). Values were calculated with the $2^{-\Delta Cp}$ method; bars correspond to standard errors. **: p.value < 0.01.

-

Figure 1.

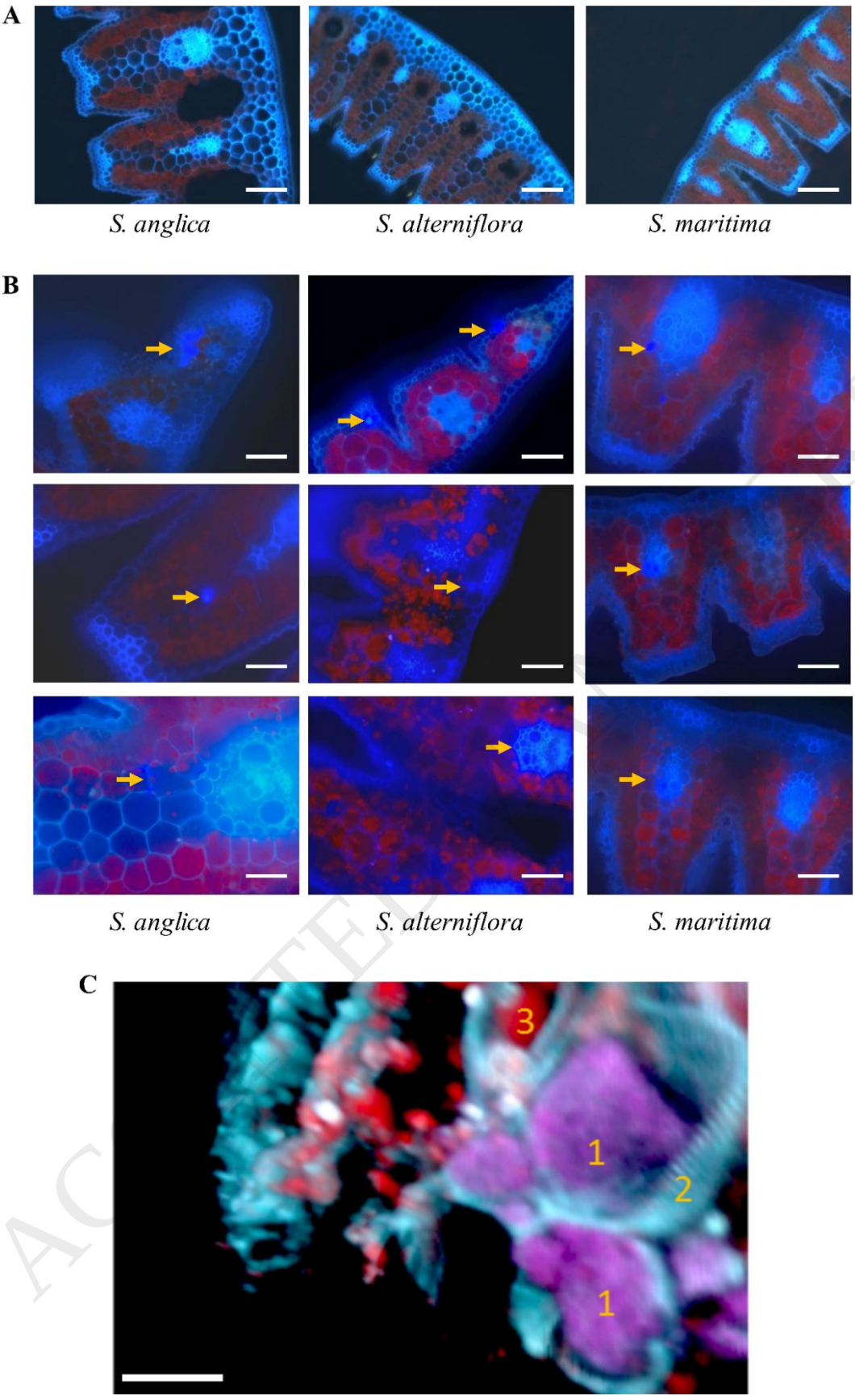

Figure 2.

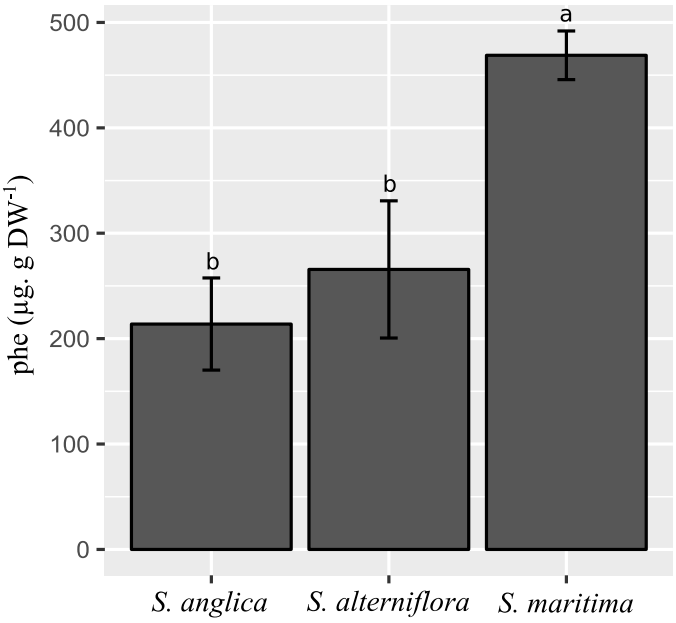

Figure 3.

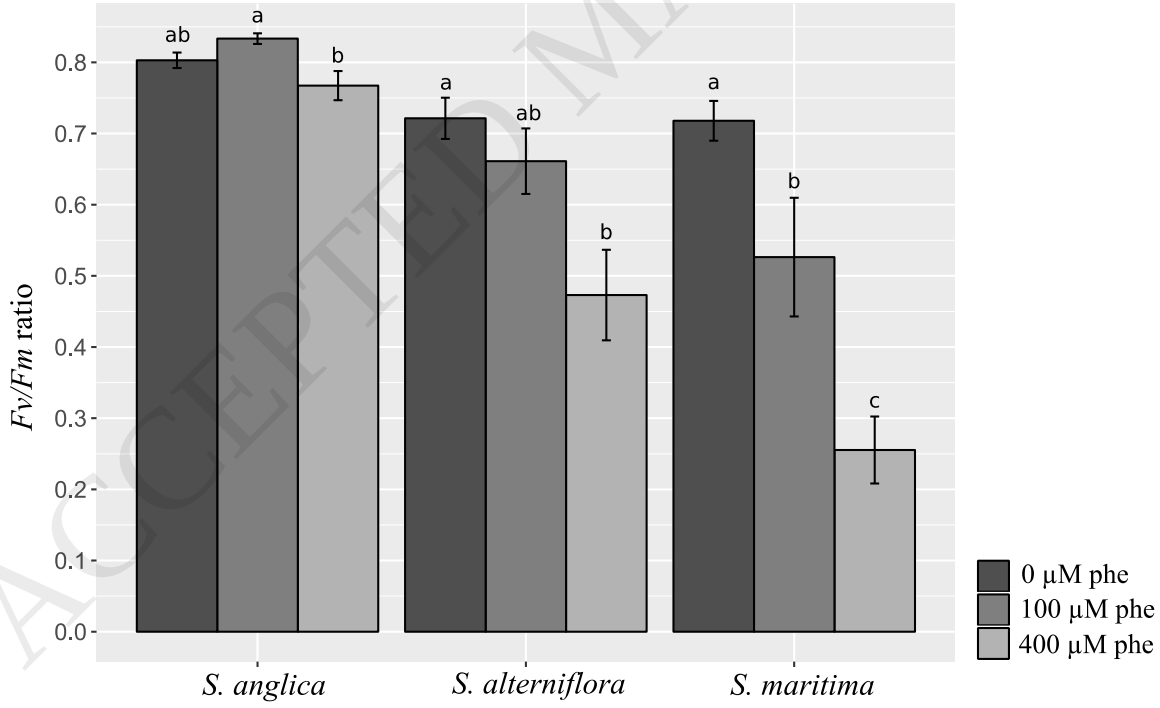

Figure 4.

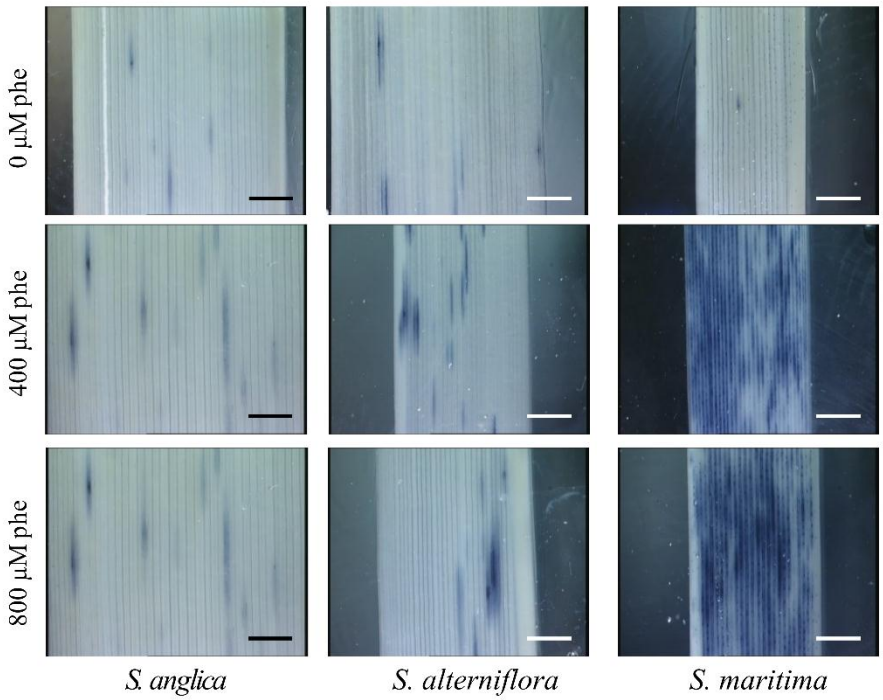

Figure 5.

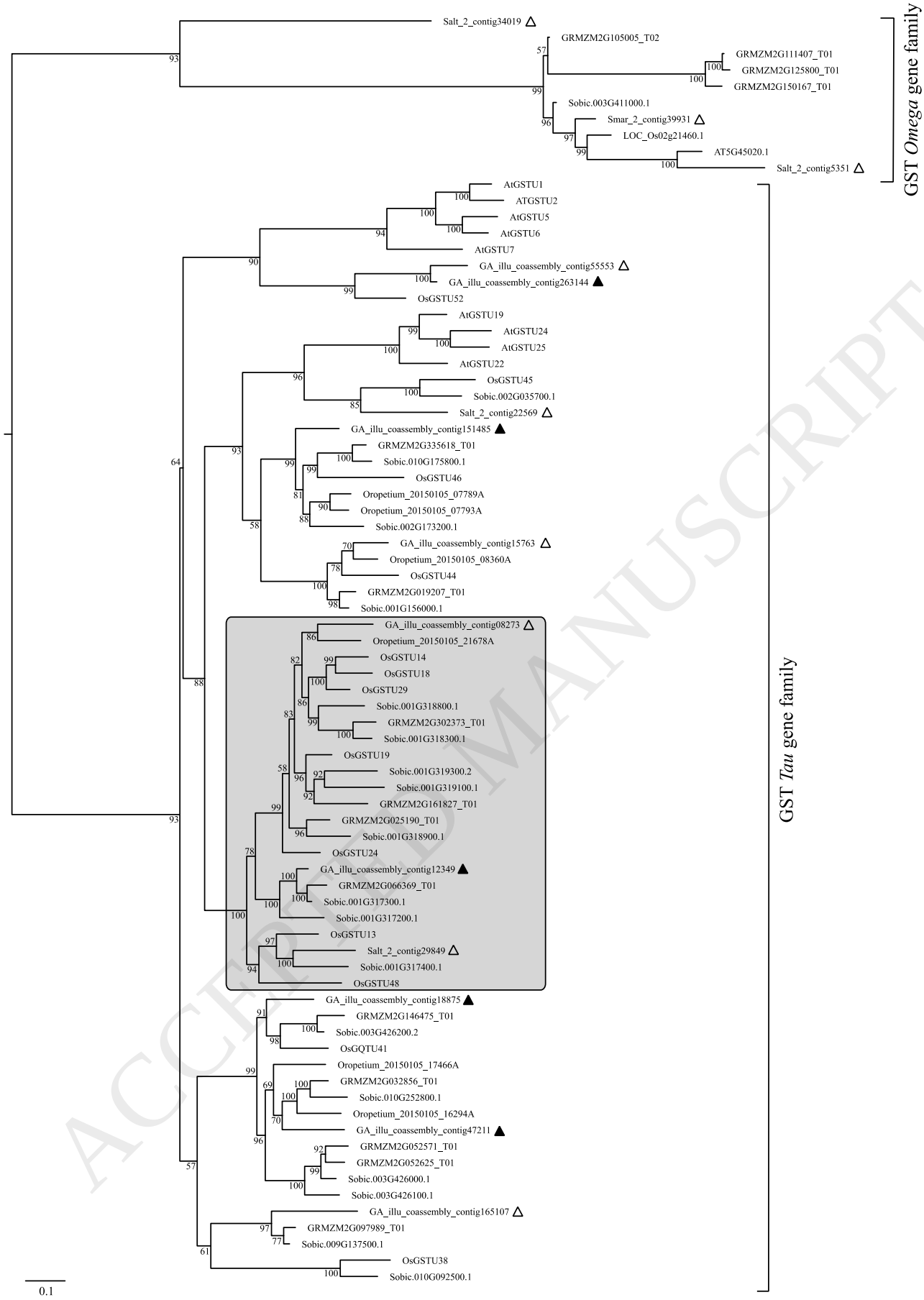

Figure 6.

A Contig GA_47211

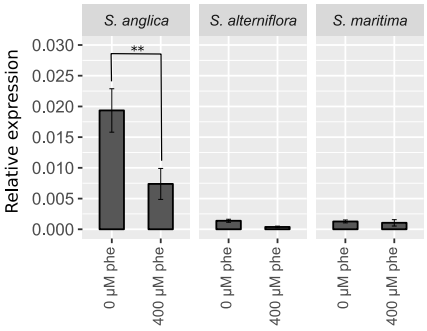

B Contig GA_151485

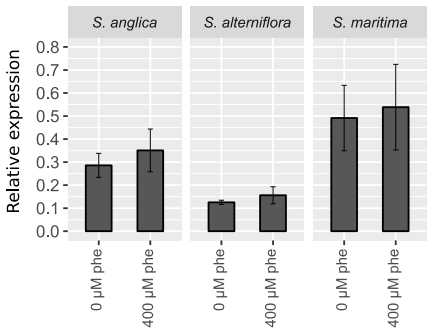

C Contig GA_12349

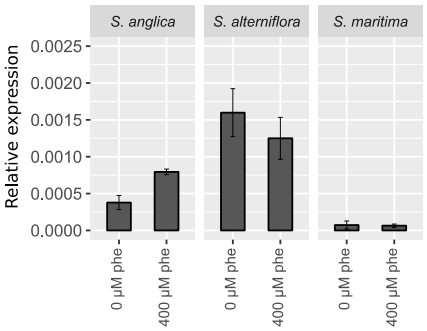

D Contig GA_15763

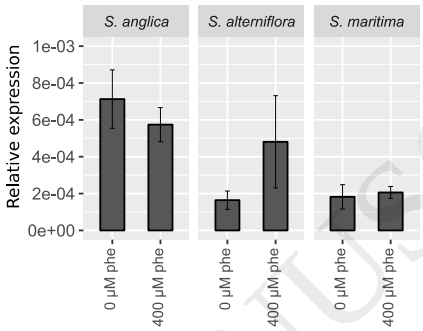

E Contig GA_263144

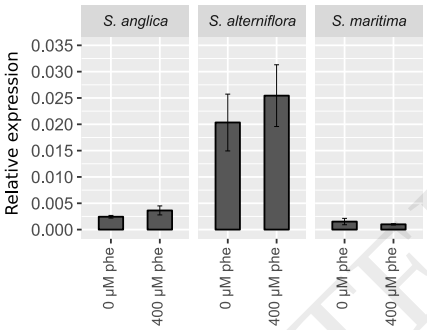

Table 1. Primers designed and validated for the six GSTs homologs in *Spartina* used for the RT-qPCR. Related *A. thaliana* genes and supplemental comments are provided.

N°	*Spartina* contigs	*A. thaliana* related homologs	Forward primer (5' → 3')	Reverse primer (5' → 3')	Supplemental comments
1	GA_47211	AtGSTU6, AtGSTU7, AtGSTU8	GATTCTGGGCCCACTTCTTC	TCGTCTCTTCCGTGAACTCC	-
2	GA_151485	AtGSTU25, AtGSTU22, AtGSTU19	GACGTAGTCTGCCCAGAAGC	AGAAGATCCCAGTGCTGCTC	-
3	GA_12349	AtGSTU14	GAGGTCCTGCTCGACGTACT	GAGGCAACTGCTAGAGCCTG	-
4	GA_02873	AtGSTU5	GAGTTTGGTGGCGCTAAATG	AGACTTGCCCTCAGCTTCAA	Deleted because of primer dimers
5	GA_15763	AtGSTU24	GACGAGGGACTCGCACAC	GTGGCGTACGAGGAGAAATC	-
6	GA_263144	AtGSTU1	AGCTGCGGCATCTGGT	TGTTCTTGAGATCCTCCTCGAT	-

Table 1.